

Electronic Supplementary Information

Uncovering the role of the ZnS treatment in the performance of Quantum Dot sensitized Solar cells

Néstor Guijarro^{1,*}, José M. Campiña¹, Qing Shen^{2,3}, Taro Toyoda², Teresa Lana-Villarreal¹,
Roberto Gómez^{1,*}

¹ *Institut Universitari d'Electroquímica i Departament de Química Física, Universitat d'Alacant, Apartat 99, E-03080 Alacant, Spain.*

² *Department of Engineering Science, Faculty of Informatics and Engineering, The University of Electro Communications, 1-5-1 Chofugaoka, Chofu, Tokyo 182-8585, Japan.*

³ *PRESTO, Japan Science and Technology Agency (JST), 4-1-8 Honcho Kawaguchi, Saitama 332-0012, Japan*

* Corresponding Authors:

Néstor Guijarro, Email: nestor.guijarro@ua.es

Roberto Gómez, Email: roberto.gomez@ua.es; Fax: +34965903537, Tel.: +34 965903748

1. Determination of the potential to carry out the photocurrent transients

The voltammograms presented in the main text (figs. 4A and 5A) have been recorded between -1.0 V and -0.6 V, while the photocurrent transients were obtained at a constant potential of -0.6 V (fig. 6). Herein we present the cyclic voltammograms for Ti(BL)/TiO₂/CdSe electrodes using a wider potential window (from -1.16 V to 0 V), both in the dark and under illumination (see figure S1A). Moreover, the voltammetric characterization in the dark is also presented for Ti(BL), Ti(BL)/TiO₂ and Ti(BL)/TiO₂/CdSe in figure S1B. As described in the experimental section, thermally treated titanium foil is employed as substrate, and taken into account that the treatment triggers the growth of a blocking layer (compact layer of TiO₂ in the surface), we refer to it as Ti(BL) in this section.

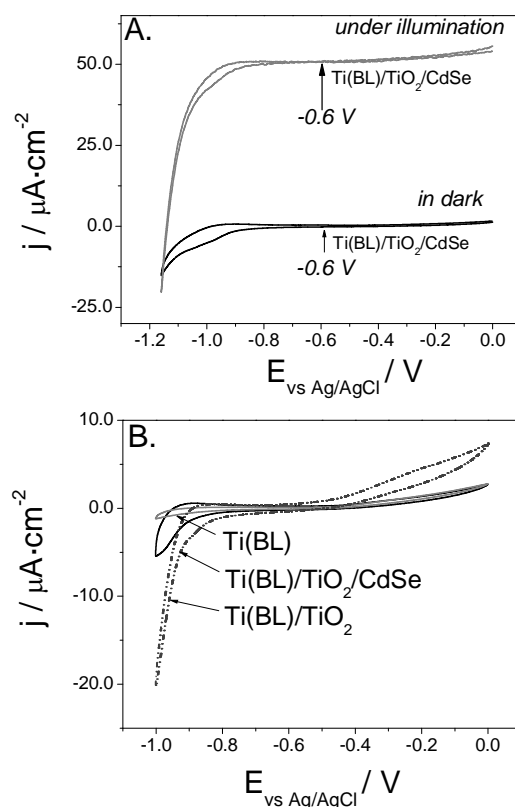


Figure S1. Cyclic voltammograms of a Ti(BL)/TiO₂/CdSe electrode in the dark and under illumination (A). Voltammograms of different electrodes: Ti(BL), Ti(BL)/TiO₂ and Ti(BL)/TiO₂/CdSe, in the dark (B). All the measurements were carried out under the conditions described in the experimental section.

As shown in figure S1A, in the dark, the current is virtually negligible at around -0.6 V, whereas at lower or higher potentials, a significant current is recorded. The cathodic current recorded at potentials lower than -0.75 V, can be mainly ascribed to the reduction of the oxidized species of the polysulfide redox couple via the TiO₂ nanoparticles, since the cathodic current measured in the bare thermally treated Ti foil is smaller (see figure S1B). On the contrary, the small anodic current recorded at potentials higher than -0.5 V is presumably due to

the oxidation of the polysulfide redox couple mainly through the TiO₂ nanoparticulate layer as inferred from figure S1B. In fact, once the TiO₂ is covered by CdSe the value of the anodic current is quite similar to that obtained for the bare thermally treated Ti foil. This is not unreasonable taking into account the efficient blockage of the TiO₂ surface by QDs discussed in the main text (see figure 4).

Under illumination (see figure S1A), the photocurrent plateau is reached at around -0.8 V with a slight increase at potentials higher than -0.5 V, due to the contribution of the dark current. Moreover, it is worth mentioning that the value of photocurrent obtained in the transient (see figure 6A) match quite well with that obtained by means of voltammetry under illumination, provided that the latter is performed at a slow scan rate (20 mV s⁻¹).

The potential of -0.6V has been selected to carry out the photocurrent transients because, on the one hand, the dark current is negligible, ensuring therefore that, the current measured under illumination is due exclusively to electron injection from the excited QDs. On the other hand, at this potential the photocurrent plateau has been reached, which guarantee that the maximum amount of electrons are collected.

2. Electrochemical Impedance Spectroscopy

2. 1 Equivalent circuit description

Figure S2 shows the Bode phase plots obtained at -1 V for different TiO₂ electrodes. Sutter et al.¹ have recently proposed a two-time-constant equivalent circuit to fit the impedance spectra obtained for self-organized TiO₂ nanotube arrays formed on titanium by anodization. A circuit constituted by two RC branches in parallel was successfully used to model the system (Figure S3). The first RC branch was ascribed to the charge transfer behavior at the semiconducting oxide/electrolyte interface and the second to relaxation via traps in the band gap. Instead of the classical capacitance, a Constant Phase Element (CPE) was included in the first branch, as it is well-known that CPEs satisfactorily account for the capacitive behavior of nanostructured thin films with large roughness and specific surface area. The resistance in this branch (R_2) accounts for the impedance of the electron transfer through this interface (referred to as R_{CT} in the article). In the second branch, R_3 is an analogous measure of charge transfer resistance, but this time via traps in the band gap. C represents the capacitance of these states. A Warburg Impedance element (W) was included by Sutter in order to get better fittings and was associated to some delay in the surface state response. Both branches are joined in series with another resistance (R_1) accounting for the electrolyte resistance. Thus, the circuit can be finally represented as $R_1[R_2Q(R_3CW)]$

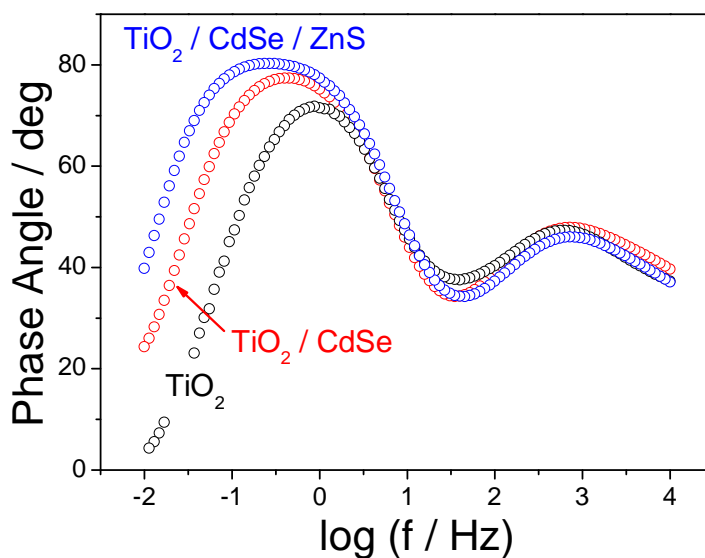


Figure S2. Bode phase plots obtained at -1 V for different TiO₂ electrodes modified or not with CdSe and ZnS. The oscillation amplitude was 10 mV. Electrolyte: 1M Na₂S + 0.1 M S + 1 M NaOH.

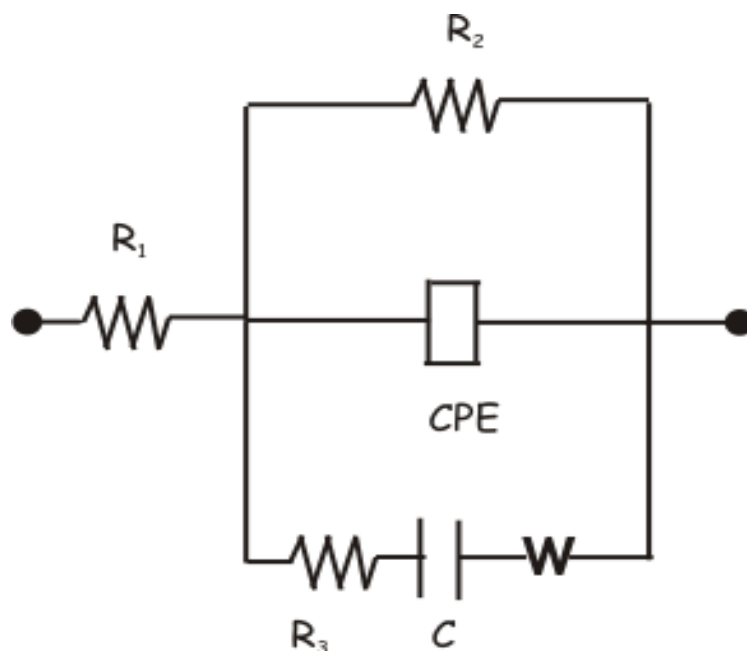


Figure S3. Equivalent circuit proposed by Sutter et al to fit the impedance data gathered for TiO_2 nanotube array films and used in this work.

As shown in our previous work,² the density of trap states strongly depends on the morphology of the investigated electrode. The evidence reported there proved that sintered nanocrystalline TiO_2 thin films possess higher concentration of band gap states when compared with single crystal or nanowire morphologies. This fact suggests the suitability of the Sutter's circuit (with one specific branch devoted to model the trap state behavior) to fit the data obtained in this work.

2.2 Fittings to the experimental EIS data.

The data fitted quite well to the $R_1[R_2Q(R_3CW)]$ circuit as shown in Figure S4.

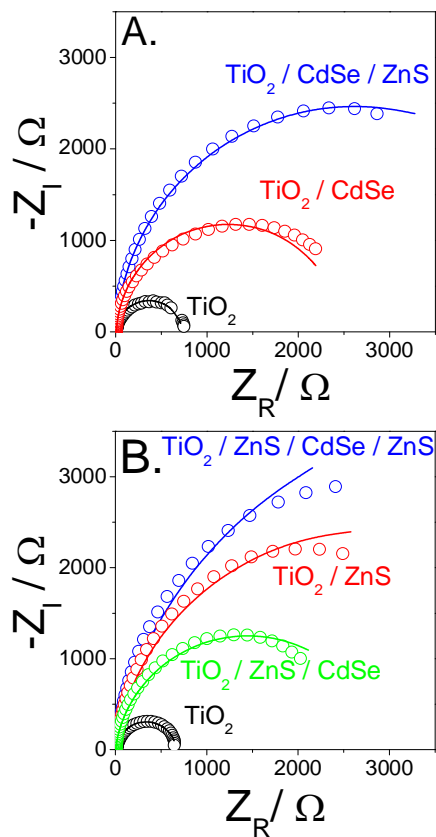


Figure S4. Nyquist plots (empty circles) and their corresponding fittings to the $R_1[R_2Q(R_3CW)]$ circuit (straight lines) for some of the modified TiO_2 electrodes. The ZnS layer was deposited after the CdSe QD deposition in (A) and also before it in (B).

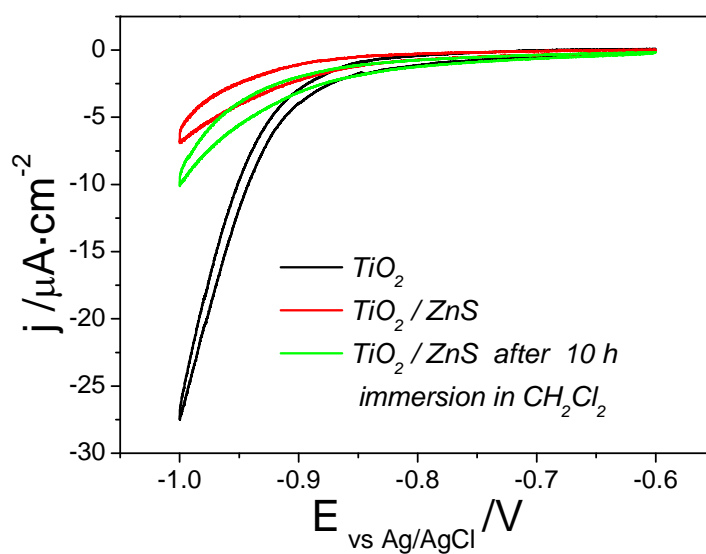


Figure S5. Voltammetric characterization of a ZnS-modified TiO_2 electrode before and after immersion in CH_2Cl_2 . The increase in cathodic current after prolonged immersion in CH_2Cl_2 suggests that a small fraction of the ZnS could detach from the TiO_2 surface. The time of immersion was 10 h, much longer than that employed for direct QD adsorption (2 h 30 min).

References

¹ P. Pu, H. Cachet and E. M. M. Sutter, *Electrochimica Acta*, 2010, **55**, 5938

² T. Berger, T. Lana-Villarreal, D. Monllor-Satoca and R. Gómez, *J. Phys. Chem. C*, 2007, **111**, 9936